JOURNAL OF COMPUTATIONAL PHYSICS 33, 405–410 (1979)

Note

Automatic Mesh-Point Clustering Near a Boundary in Grid Generation with Elliptic Partial Differential Equations

In finite difference techniques, one practical way of treating boundary data that are specified along an arbitrary curve is to map the boundary curve onto a grid coordinate line. Various schemes are available to achieve such mappings, including conformal mapping [1, 2], shearing transforms, algebraic schemes [3], and elliptic partial differential equations that satisfy a maximum principle [4–9]. Of these, the elliptic equation technique appears the most flexible for generating well-ordered finite difference grids about arbitrary two- and three-dimensional surfaces.

Elliptic partial differential equations can be used to generate a smooth grid that permits a one-to-one mapping so that mesh lines of the same family do not cross. However, the grid so generated is not always satisfactory in the sense that points may not be clustered to where they are needed, or mesh lines of the opposite family may intersect at highly acute angles. To correct this deficiency, various forcing or source terms are used that are either compatible with the maximum principle or that are so controlled locally that mesh lines cannot intersect. In particular, Thompson *et al.* [9] have proposed as governing equations

$$\begin{aligned} \xi_{xx} + \xi_{yy} &= P(\xi, \eta), \\ \eta_{xx} + \eta_{yy} &= Q(\xi, \eta), \end{aligned} \tag{1}$$

where the forcing terms are defined as

$$P = -\sum_{m=1}^{M} a_m \frac{\xi - \xi_m}{|\xi - \xi_m|} e^{-c_m|\xi-\xi_m|} - \sum_{i=1}^{I} b_i \frac{\xi - \xi_i}{|\xi - \xi_i|} e^{-d_i[(\xi-\xi_i)^2+(\eta-\eta_i)^2]^{1/2}},$$

$$Q = -\sum_{m=1}^{M} a_m \frac{\eta - \eta_m}{|\eta - \eta_m|} e^{-c_m|\eta-\eta_m|} - \sum_{i=1}^{I} b_i \frac{\eta - \eta_i}{|\eta - \eta_i|} e^{-d_i[(\xi-\xi_i)^2+(\eta-\eta_i)^2]^{1/2}}.$$

0021-9991/79/120405-06$02.00/0

In the transformed space, these equations are written as

$$\begin{aligned} \alpha x_{\xi\xi} - 2\beta x_{\xi\eta} + \gamma x_{\eta\eta} &= -J^2(Px_\xi + Qx_\eta), \\ \alpha y_{\xi\xi} - 2\beta y_{\xi\eta} + \gamma y_{\eta\eta} &= -J^2(Py_\xi + Qy_\eta), \end{aligned} \tag{2}$$

where J is the transform Jacobian $J = x_\xi y_\eta - x_\eta y_\xi$ and

$$\alpha = x_\eta^2 + y_\eta^2, \qquad \beta = x_\xi x_\eta + y_\xi y_\eta, \qquad \gamma = x_\xi^2 + y_\xi^2.$$

The difficulty with the above forcing terms is that no automatic way has been available to choose the coefficients of P and Q for a desired clustering, although various approximate techniques have been developed [8, 9]. For the most part, the P and Q terms are selected to achieve two main effects: (1) to cluster points to a boundary, and (2) to force grid lines to intersect the boundary in a nearly normal fashion. The purpose of this note is to show that these two effects can be achieved automatically for smooth boundary curves by adding boundary relations to the governing equations.

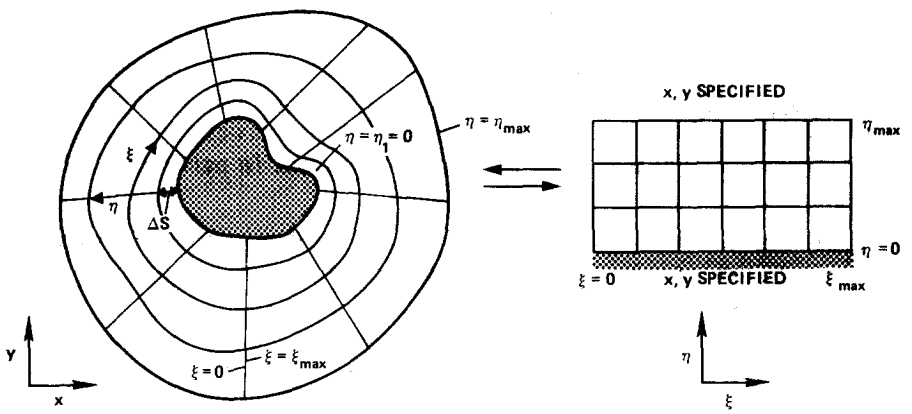

FIG. 1. Schematic of grid showing terminology.

The present approach restricts the application of the forcing terms to the inner boundary ($\eta = \eta_1$) of Fig. 1, which simplifies the governing equations to

$$\alpha x_{\xi\xi} - 2\beta x_{\xi\eta} + \gamma x_{\eta\eta} = -J^2(P_1 e^{-a(\eta-\eta_1)} x_\xi + Q_1 e^{-b(\eta-\eta_1)} x_\eta), \tag{3a}$$

$$\alpha y_{\xi\xi} - 2\beta y_{\xi\eta} + \gamma y_{\eta\eta} = -J^2(P_1 e^{-a(\eta-\eta_1)} y_\xi + Q_1 e^{-b(\eta-\eta_1)} y_\eta), \tag{3b}$$

where $P_1 = P(\xi, \eta_1)$, $Q_1 = Q(\xi, \eta_1)$, and a and b are specified positive constants.

In the notation of Fig. 1, the first condition that we want to satisfy simply states that we want to control the spacing between the η_1 (i.e., boundary) coordinate line and the adjacent η_2 coordinate line. The elliptic governing equations are relied upon

to maintain continuity or smoothness between the lines η_1, η_2, η_3, ... That is, if s is the distance along a ξ = constant coordinate, we want to specify Δs at the boundary $\eta = \eta_1$. Now

$$\Delta s \doteq [(\Delta x)^2 + (\Delta y)^2]^{1/2}\,|_{\xi=\text{const}} \tag{4}$$

and in the limit

$$\begin{aligned} ds &= [(dx)^2 + (dy)^2]^{1/2} \\ &= [(x_\xi\, d\xi + x_\eta\, d\eta)^2 + (y_\xi\, d\xi + y_\eta\, d\eta)^2]^{1/2}. \end{aligned}$$

Or, because ξ is constant along the η-coordinate,

$$ds = [(x_\eta)^2 + (y_\eta)^2]^{1/2}\, d\eta\,|_{\xi=\text{const}}. \tag{5}$$

To enforce the second condition that grid lines intersect the body in a nearly normal fashion, we use the general relation

$$\nabla\xi \cdot \nabla\eta = |\,\nabla\xi\,|\,|\,\nabla\eta\,|\cos\theta, \tag{6}$$

where θ equal to $\pi/2$ yields orthogonality. Using the transform relations $\xi_x = y_\eta/J$, etc., we can rewrite Eq. (6) as

$$x_\xi x_\eta + y_\xi y_\eta = -[x_\eta^2 + y_\eta^2)(x_\xi^2 + y_\xi^2)]^{1/2}\cos\theta. \tag{7}$$

Along the $\eta = \eta_1$ boundary, x and y are specified so all derivatives in ξ are known (i.e., x_ξ, y_ξ, $x_{\xi\xi}$, etc., are given) and are assumed continuous. Relations (5) and (7) determine x_η and y_η as well

$$x_\eta = s_\eta(-x_\xi\cos\theta - y_\xi\sin\theta)/(x_\xi^2 + y_\xi^2)^{1/2}, \tag{8a}$$

$$y_\eta = s_\eta(-y_\xi\cos\theta + x_\xi\sin\theta)/(x_\xi^2 + y_\xi^2)^{1/2}, \tag{8b}$$

where θ and $s_\eta = (ds/d\eta)\,|_\xi$ are specified functions of ξ and the sign conventions were chosen for ξ positive clockwise and for η positive radially outward as shown in Fig. 1. The cross-derivative terms along the boundary are also known once x_η and y_η are known as functions of ξ. Thus at the $\eta = \eta_1$ boundary all of the terms in Eq. (3) are known except for P_1, Q_1, $x_{\eta\eta}$, and $y_{\eta\eta}$. However, x and y are known on the boundary, so $x_{\eta\eta}$ and $y_{\eta\eta}$ on the boundary are determined from the simultaneous solution of Eqs. (3) for x and y in the interior field. Therefore, evaluation of Eqs. (3) on the boundary yields two independent equations for finding P_1 and Q_1

$$P_1 = J^{-1}(y_\eta R_1 - x_\eta R_2)\,|_{\eta=\eta_1}, \tag{9a}$$

$$Q_1 = J^{-1}(-y_\xi R_1 + x_\xi R_2)\,|_{\eta=\eta_1}, \tag{9b}$$

where

$$R_1 = -J^{-2}(\alpha x_{\xi\xi} - 2\beta x_{\xi\eta} + \gamma x_{\eta\eta})\,|_{\eta=\eta_1},$$

$$R_2 = -J^{-2}(\alpha y_{\xi\xi} - 2\beta y_{\xi\eta} + \gamma y_{\eta\eta})\,|_{\eta=\eta_1},$$

and where Eq. (9) uses a simplification of Eq. (3) insofar as $\eta = \eta_1$ so

$$e^{-a(\eta-\eta_1)} = e^{-b(\eta-\eta_1)} = 1.$$

Simple relaxation routines have been used to solve Eqs. (3) and (9). Successive line overrelaxation (SLOR) is used to solve Eq. (3) over the exterior field where the left-hand side terms are all centrally differenced. Because the forcing term coefficients P_1 and Q_1 can be quite large, the derivatives x_ξ, x_η, y_ξ, and y_η of the forcing terms can cause instability if they are centrally differenced (see, for example, [10] for related analysis). Consequently, the usual trick [10–12] of backward or forward differencing of these terms is used, i.e., if P_1 is positive, x_ξ is approximated with $(x_{j+1} - x_j)/\Delta\xi$, while if P_1 is negative, x_ξ is approximated with $(x_j - x_{j-1})/\Delta\xi$, etc. Along the surface

$$x_{\eta\eta} = (-7x_1 + 8x_2 - x_3)/(2\Delta\eta^2) - 3x_\eta\,|_1/\Delta\eta, \tag{10a}$$

$$y_{\eta\eta} = (-7y_1 + 8y_2 - y_3)/(2\Delta\eta^2) - 3y_\eta\,|_1/\Delta\eta, \tag{10b}$$

where x_1, y_1, $x_\eta\,|_1$, and $y_\eta\,|_1$ are specified. At $\eta = \eta_1$, P_1 and Q_1 are updated after each SLOR sweep of the field from

$$P_1^{(n+1)} = P_1^{(n)} + \omega_P[J^{-1}(y_\eta R_1 - x_\eta R_2)^{(n+1)} - P_1^{(n)}], \tag{11a}$$

$$Q_1^{(n+1)} = Q_1^{(n)} + \omega_Q[J^{-1}(-y_\xi R_1 + x_\xi R_2)^{(n+1)} - Q_1^{(n)}], \tag{11b}$$

where n is the iteration level. As in [10], where similar boundary conditions are

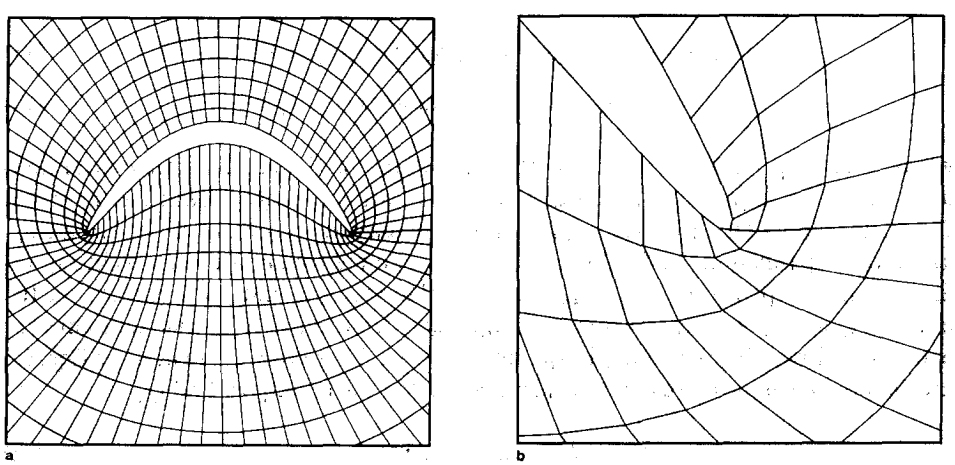

FIG. 2. Unclustered grid about highly cambered airfoil. (a) Grid detail about airfoil (outer boundary not shown). (b) Grid detail at trailing edge.

imposed, ω_P and ω_Q are very small (ω_P , $\omega_Q = 0.02 \rightarrow 0.06$). Also, even for very small ω_P and ω_Q the corrections predicted by Eq. (11) can be too large during the early stages of the relaxation scheme if a poor guess is used, so the change in P_1 and Q_1 is limited to a small percentage of their previous values.

Our automatic clustering technique has been successfully used to generate various airfoil grids. For example, Fig. 2 shows the grid generated with P_1 and $Q_1 = 0$ about a highly cambered airfoil whose basic thickness distribution is a 12 to 1 ellipse. The grid spacing on the lower surface is clearly inadequate, especially for viscous flow calculations. Figure 3 shows a grid where orthogonality is imposed and a constant value of $ds = 0.005$ was specified along the entire airfoil. In this case, the chord of the airfoil is 1 (i.e., the length in x is 1); so $ds = 0.005$ means that Δs is approximately equal to 1/200 of the chord. Values for ds as small as 0.00001, which are needed for high Reynolds number viscous flow calculations, are just as easy to compute, but the details are lost in a plot such as Fig. 3 because the inner lines blur together. We remark that the ds grid spacing that we impose is not exactly equal to the computed grid spacing Δs because the differential relations are exact only in the limit. However, the closeness, which is more than adequate, improves as Δs is refined. Comparisons of Figs. 2b and 3b clearly illustrate the effect of imposing orthogonality at the trailing edge.

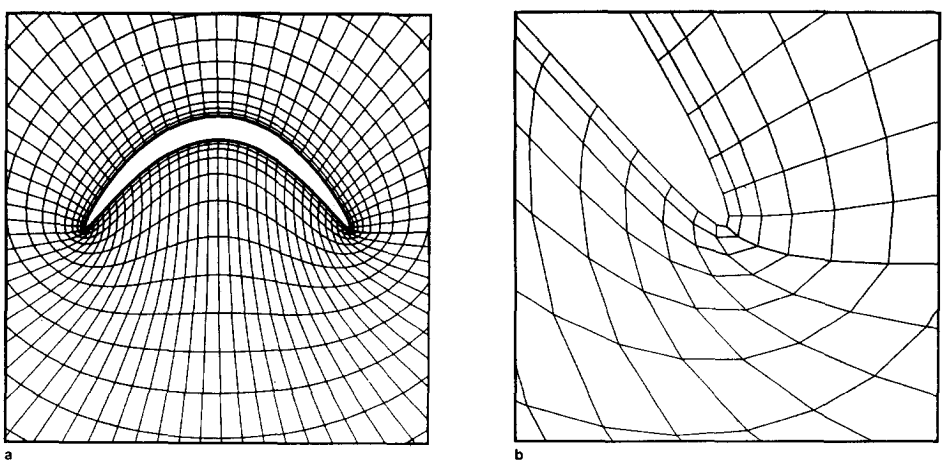

FIG. 3. Clustered grid with orthogonality imposed at airfoil surface using exponential coefficients of $a = b = 1$. (a) Grid detail about airfoil. (b) Grid detail at trailing edge showing surface orthogonality and uniform clustering.

In closing, we remark that, if a poor initial guess of P_1 and Q_1 is used, some 400 to 800 iterations of the relaxation algorithm are needed to generate a grid such as that in Fig. 3. Thus, a more efficient relaxation algorithm for the combined Eqs. (3) and (9) will be needed for many grid generation applications. As obvious extensions of this procedure, we note that additional forcing terms can be added at the other boundary surfaces (and indeed have already been added in one-dimensional applications).

REFERENCES

1. D. C. IVES, *AIAA J.* **14** (1976), 1006.
2. G. MORETTI, "Extended Conformal Mappings for Supersonic Aircraft Calculations," Poly-AG/AM Rep. No. 76–8, 1976.
3. P. A. EISEMAN, *J. Computational Physics* **26** (1978), 307.
4. A. M. WINSLOW, *J. Computational Physics* **2** (1967), 149.
5. W. H. CHU, *J. Computational Physics* **8** (1971), 392.
6. S. K. GODUNOV AND G. P. PROKOPOV, *USSR Comp. Math. Phys.* **12** (1972), 182.
7. J. F. THOMPSON, F. C. THAMES, AND C. M. MASTIN, *J. Computational Physics* **15** (1974), 299.
8. U. GHIA, J. K. HODGE, AND W. L. HANKEY, Air Force Flight Dynamics Laboratory AFFDL-TR-77-117, 1977.
9. J. F. THOMPSON, F. C. THAMES, AND C. W. MASTIN, *J. Computational Physics* **24** (1977), 274.
10. J. M. KLINEBERG AND J. L. STEGER, NASA TN D-7332, 1974.
11. P. J. ROACHE, "Computational Fluid Dynamics," Hermosa, Albuquerque, N. Mex., 1972.
12. M. ATIAS, M. WOLFSTEIN, AND M. ISRAELI, *in* Proceedings, AIAA 2nd Computational Fluid Dynamics Conference, 1975.

RECEIVED: October 4, 1978; REVISED: February 1, 1979

J. L. STEGER AND R. L. SORENSON

NASA Ames Research Center
Moffett Field, California 94035